Asian Journal of Chemistry; Vol. 27, No. 2 (2015), 657-662

ASIAN JOURNAL OF CHEMISTRY

http://dx.doi.org/10.14233/ajchem.2015.17447

Removal of Fluoride from Aqueous Solution by Adsorption onto Attapulgite Supported CeO_2 Nanoparticles

JIAHONG WANG[1,*], E. CHANG[1] and YANFEN JI[2]

[1]College of Resource and Environment, Shaanxi University of Science and Technology, Xi'an 710021, P.R China
[2]State Key Laboratory of Pollution Control and Resource Reuse and School of the Environment, Nanjing University, Nanjing 210093, P.R China

*Corresponding author: Tel: +86 29 86168291; E-mail: wangjiahong@sust.edu.cn

Received: 22 February 2014; *Accepted*: 19 May 2014; *Published online*: 10 January 2015; AJC-16641

Attapulgite supported CeO_2 (ATP-CeO_2) was prepared and characterized by FTIR, XRD, TEM and zeta potential measurement. ATP-CeO_2 exhibits high adsorption capacity for aqueous fluoride and fluoride adsorption amount onto ATP-CeO_2 decreased with rise in solution pH and electrostatic interaction and anionic exchange may contribute to the enhanced fluoride adsorption. The presence of anions in solution suppressed fluoride adsorption by competing with fluoride ions for the active sites of the adsorbent surface. Adsorption isotherms of fluoride can be well described by Langmiur model and the maximum adsorption amount were 14.97, 18.08 and 22.42 mg/g at 15, 25 and 35 °C, respectively and fluoride adsorption onto ATP-CeO_2 increased with increasing adsorption temperature, indicating of an endothermic process. Pseudo-second order kinetic equation can fit the fluoride adsorption satisfactorily. Fluoride saturated ATP-CeO_2 can be easily desorbed in 0.1 mol/L NaOH solution and regenerated adsorbents still showed high adsorption amount for fluoride in water.

Keywords: Defluoridation, Attapulgite Supported Cerium oxide, Kinetics, Adsorption, Regeneration.

INTRODUCTION

Fluoride pollution was widely found in industrial wastewater derived from metal finishing and electroplating, aluminum and steel production, glass and semiconductor manufacturing, ore beneficiation and fertilizer operation. Fluoride in water may be a great threat to human health because of their possible accumulation and damage to the human tissues. According to the World Health Organization, the tolerance limits of fluoride in drinking water is 1.5 mg/L. Excessive exposure to fluoride may result in mottling of teeth, softening of bones, even neurological damages[1-3]. Therefore, it is necessary to eliminate the excessive fluoride from drinking water.

Various methods, such as membrane filtration[4], precipitation[5], adsorption[6], ion exchange[7,8], electrodialysis[9], electrochemical methods[10], *etc.* have been developed to remove fluoride from aqueous solution. Among these, adsorption is still considered as one of the most extensively used methods because of its high efficiency and simple operation. Activated carbon[11], bone charcoal[12], zeolites[13], resin, *etc.* have been reported to show high adsorption capacity for fluoride in aqueous solution, but they are usually too expensive. In recent years, increasing attentions of researchers have been devoted to develop the low cost adsorbents such as natural clays, minerals, metal oxides and industrial or agricultural wastes.

Attapulgite is a kind of hydrated magnesium aluminium silicate mineral with fibrillar morphology and attapulgite resource is abundant in China. As a nano-clay mineral, attapulgite have the large specific surface area, porous structure and moderate cation exchange capacity, which exhibits strong affinity for metal cations such as Cd(II), Cu(II), Pb(II), Hg(II), *etc.*[14-16]. However, adsorption capacity of anionic pollutants onto attapulgite is not satisfactory because its negatively charged surface suppresses the adsorption of anions. Attapulgite adsorbents modified with metal salts such as magnesium, aluminum and zirconium salts, have been found to exhibit high adsorption affinity for fluoride in aqueous solution[17,18].

Recent researches show that various rare earth elements, such as Ce(IV) oxides, are very effective in removal of fluoride from aqueous solution. For example, Al-Ce hybrid adsorbent[19], Fe-Ce adsorbent, Fe-Al-Ce trimetal oxide adsorbent[20-22], Mn-Ce oxide adsorbent[23], aligned carbon nanotubes supported ceria nanopariticles[24], Ti-Ce hybrid oxide[25], Ce(III)-loaded amberlite resin[26], Ce(III) encapsulated chitosan polymeric matrix[27], activated cerium(IV) oxide/SiMCM-41 adsorbent[28] and CeO_2-TiO_2/SiO_2 composites[29], have been reported to show high adsorption capacity for fluoride in aqueous solution. Therefore, attapulgite supported CeO_2 nanoparticles (ATP-CeO_2) may be used as an effective adsorbent for the removal of fluoride from aqueous solution. Nevertheless, to our best of knowledge, no

studies have been made to apply the ATP-CeO_2 to eliminate the aqueous fluoride.

In this study, the ATP-CeO_2 adsorbent was prepared by homogeneous precipitation. The structural and physico-chemical properties of the adsorbent were characterized by FTIR, TEM and XRD analysis. The adsorption of fluoride in solution onto ATP-CeO_2 was conducted by batch experiments and kinetic tests. Effect of solution chemistry conditions including solution pH and competing anions were also studied and the possible sorption mechanisms were discussed.

EXPERIMENTAL

Attapulgite nano-fibrillar clay with the average diameter of 100 meshes was provided by Jiangsu Huida Co. Ltd., Jiangsu, China. Hexamethylenetetramine ($C_6H_{12}N_4$), $Ce(NO_3)_3{\cdot}6H_2O$ were purchased from Sinopharm Chemical Reagent Co., Ltd. (China). All chemicals and reagents were of analytical grade and used without pretreatment. 1000 mg/L fluoride stock solution was prepared by dissolving NaF in 1 L of deionized water from a Milli-Q water system.

Adsorbent preparation: ATP-CeO_2 adsorbent was synthesized by homogeneous precipitation. 5 g attapulgite and 6.35 g $Ce(NO_3)_3.6H_2O$ was dispensed in 100 mL deionized water and sonicated for 15 min, then stirred magnetically for 1 h at room temperature. 10.25 g of hexamethylene tetramine was added to the mixture and reacted for 2 h at 70 °C under magnetic stirring. The contents were cooled to room temperature, then filtrated and washed by deionized water till neutralization. The resulting solid was drying at 80 °C for 8 h and calcined at 250 °C for 2 h and then the adsorbent of attapulgite supported CeO_2 was obtained. The pure CeO_2 nanoparticles were synthesized by the above method in absence of attapulgite addition.

Adsorbent characterization: Fourier transform-infrared spectra were recorded in a FT-IR spectrometer (Bruker, Germany) at 2 cm^{-1} resolution. X-ray diffraction patterns of the samples were recorded on a powder diffraction meter with a Cu anode at 40 KV and 40 mA in the range of 3-60°, with a speed of 2 min^{-1}. TEM observations were performed on a transmission electron microscope (JEOL, Japan). Zeta potentials of ATP, ATP-CeO_2 and CeO_2 particles were measured using a zeta potential analyzer (Zeta PALS, Brookhaven Instruments Co., USA). Solution pH was adjusted with 0.1 mol/L HCl and NaOH.

Adsorption tests: Batch-wise sorption study was carried out for fluoride at 15, 25 and 35 °C. Briefly, 20 mg ATP-CeO_2 was added to 40 mL flask receiving 40 mL of fluoride solution with initial concentrations from 5 to 60 mg/L with pH 6. The flasks were transferred into an incubator and shaken for 4 h. After achieving to adsorption equilibrium, the adsorbent was filtrated by 0.45 membrane filter and the residual concentrations of fluoride in solution were measured by a fluoride meter equipped with fluoride ion selective electrode.

The influence of pH on fluoride onto ATP-CeO_2 was studied by adjusting fluoride solutions (50 mg/L) to different pH values varying from 2 to 11 preadjusted by 0.1 mol/L NaOH or HCl and shaking 50 mL of fluoride solution with 20 mg of adsorbent at 25 °C for 4 h. Effect of the competing anions on fluoride adsorption was studied by dispensing 20 mg of adsorbents in 40 mL Cl^-, NO_3^-, SO_4^{2-}, or CO_3^{2-} solution (5-25 mg/L) containing 50 mg/L fluoride ion at pH 6.

For adsorption kinetics at 25 °C, 200 mg of ATP-CeO_2 was fast introduced into a 500 mL three neck flask receiving 500 mL of fluoride solution at an initial fluoride ion concentration of 10, 30 and 50 mg/L, respectively, under strong magnetic stirring. At a certain time intervals, 4 mL of solution was withdrawn and filtrated for the residual fluoride ion concentration tests.

Desorption and regeneration: For batch desorption study, 100 mg ATP-CeO_2 was dispensed in 50 mL flask receiving 40 mL 50 mg/L fluoride solution and shaken for 4 h. Fluoride ion saturated ATP-CeO_2 was separated by centrifugation and washed gently with water to remove unadsorbed fluoride ion. Then fluoride ion loaded adsorbent was dispensed in 25 mL of 0.1 mol/L NaOH and shaken for 2 h. The regenerated ATP-CeO_2 was separated centrifugally and washed thoroughly with deionized water for following experiment. The adsorption-regeneration cycles were repeated for four times.

RESULTS AND DISCUSSION

Adsorbent characterization: The FTIR spectra of ATP and ATP-CeO_2 are shown in Fig. 1. As illustrated in Fig. 1, for ATP, the main characteristic peak at 1032 cm^{-1} is attributed to stretching vibration of Si-O-Si. The band at 1640 cm^{-1} is ascribed to the bending vibration of adsorbed water (H-O-H) and the broad band at 3400 cm^{-1} corresponds to the stretching vibration of hydroxyl (-OH). But for ATP-CeO_2, apart from the above characteristic bands, a new band at 1396 cm^{-1} corresponded to the banding mode of Ce-O was observed, which indicated that CeO_2 was coated on the surface of ATP.

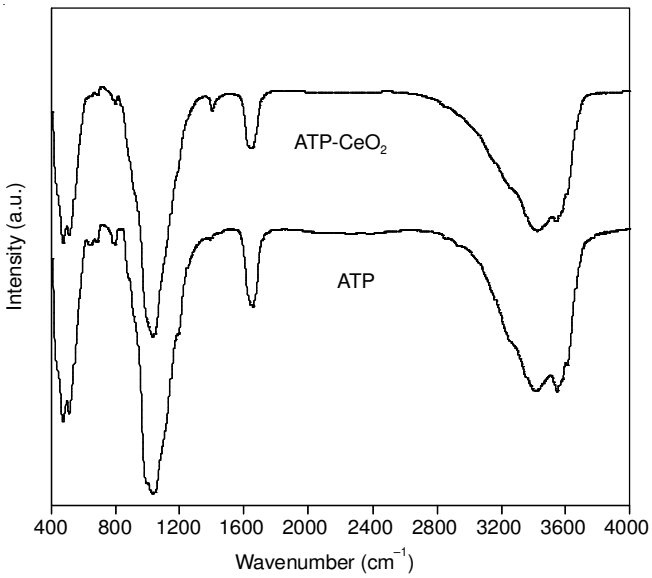

Fig. 1. FTIR spectra of free ATP and ATP-CeO_2

The crystal structures of ATP and ATP-CeO_2 are characterized by XRD patterns and results are shown in Fig. 2. For ATP, the typical diffraction peaks at 2θ = 8.3, 13.8, 19.7 and 27.3 is in good agreement to the primary diffraction of the (110), (200), (040) and (400) planes of ATP. After the coating

of CeO_2 nanoparticles, several new diffraction peaks appeared at 2θ = 28.4, 47.4 and 56.4, corresponded to the (111), (220) and (311) planes of cubic fluorite structure of CeO_2, indicating of the formation of ATP-CeO_2 composite[30].

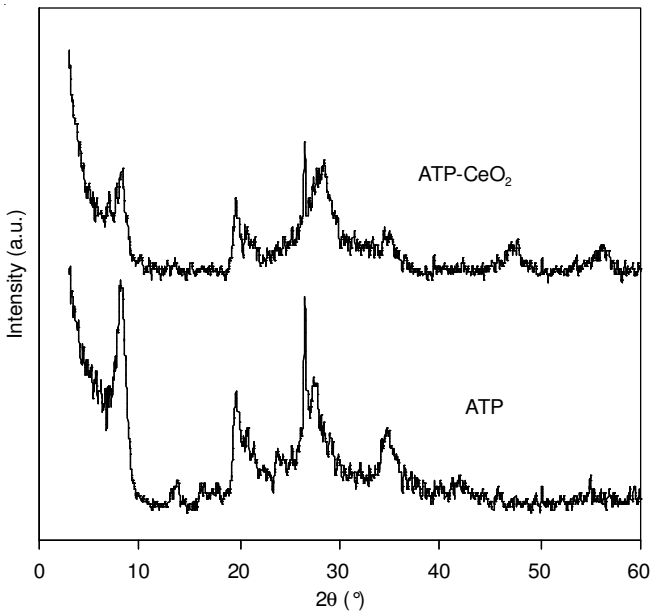

Fig. 2. XRD patterns of free ATP and ATP-CeO_2

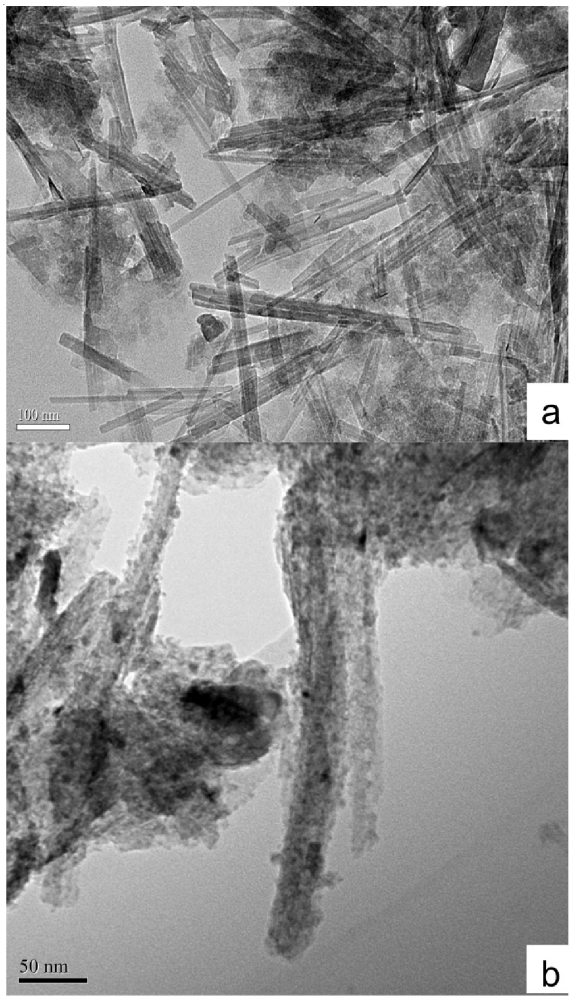

Fig. 3. TEM image of ATP (a) and ATP-CeO_2 (b)

Successful coating of CeO_2 nanoparticles on ATP was further confirmed by TEM observation. The TEM images of ATP and ATP-CeO_2 are illustrated in Fig. 3. From the Fig. 3a, raw ATP clay is a typical fibrillar single crystal with the diameter of 10-25 nm. After coating of CeO_2 (in Fig. 3b), CeO_2 nanoparticles with particle size of 3-8 nm was distributed uniformly on the surface of ATP needles.

The surface charge of ATP, ATP-CeO_2 and CeO_2 measured as zeta potential are illustrated in Fig. 4. The isoelectric point (IEP) of ATP was found to be less than 1.0, however, the isoelectric point of ATP-CeO_2 and pure CeO_2 are 2.7 and 6.1, which indicates that CeO_2 was successfully covered on the surface of ATP.

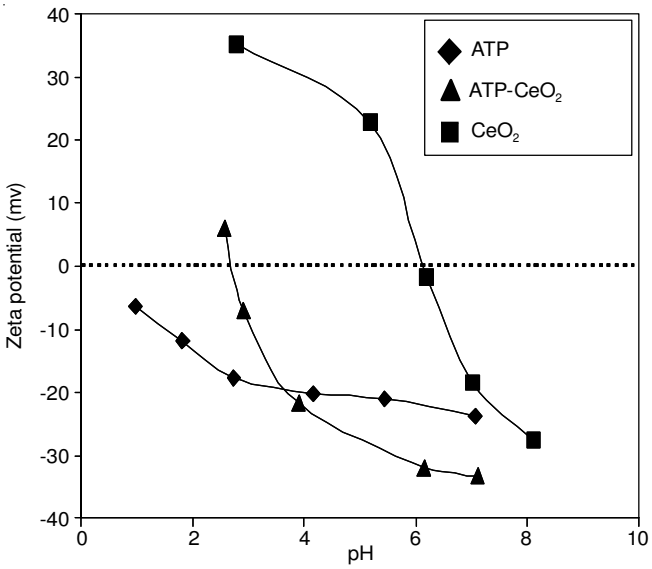

Fig. 4. Zeta potentials of ATP, ATP-CeO_2 and CeO_2 as a function of solution pH

Influence of solution pH: Solution pH is an important parameter to affect the adsorption of fluoride ion on adsorbents because the surface chemical properties of adsorbents vary with the change of solution pH. Effect of solution pH on fluoride adsorption onto ATP-CeO_2 was depicted in Fig. 5. From the results, fluoride adsorption amount decreased monotonously with increasing solution pH, which may be attributed

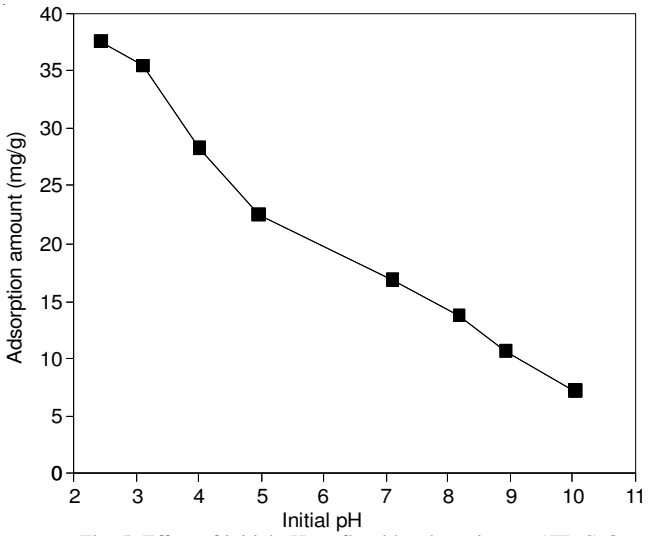

Fig. 5. Effect of initial pH on fluoride adsorption on ATP-CeO_2

to the change of surface charge of ATP-CeO_2. Generally, in aqueous solution, the surface hydroxyl groups would be formed on metal oxide by hydrolysis reaction between the metal oxide and water. Therefore, the ATP-CeO_2 surface also has hydroxyl groups, which can accept or provide different amounts of protons at different pH and form ATP-$CeOH_2^+$, ATP-CeOH and ATP-CeO^- groups on the adsorbent surface.

From the result in Fig. 4, the isoelectric point of CeO_2 is at pH 6.1, which suggests that at pH below 6.1, the surface of ATP-CeO_2 is charged positively and ATP-$CeOH_2^+$ groups existed on the adsorbent surface. The strong electrostatic interaction between ATP-$CeOH_2^+$ and fluoride ions would be awoken, which led to the enhanced fluoride adsorption at lower pH. While at pH above 6.1, the adsorbent surface has the negative charge and further decreased with increasing solution pH, whereas the electric repulsion between the adsorbent surface and fluoride ions tended to repel the fluoride ions and led to the decrease of fluoride adsorption. Additionally, in alkaline solution, hydroxyl ions would compete with fluoride on the active adsorption sites, which may be another reason for the decreased fluoride adsorption.

The pH changes before and after fluoride adsorption at different initial solution pH was observed in Table-1. Solution pH after fluoride adsorption was improved at lower pH and decreased at higher pH, which may be explained by the surface reactions of ATP-CeO_2. In aqueous solution of fluoride adsorption, the following two reactions are coexisted as follows:

$$\text{ATP-CeOH} + H_2O + F^- \rightleftharpoons \text{ATP-CeOH}_2^+ + F^- + OH^- \rightleftharpoons \text{ATP-CeOH}_2\text{-F} + OH^- \rightleftharpoons \text{ATP-CeF} + OH^- + H_2O \quad (1)$$

$$\text{ATP-CeOH} + H_2O + Na^+ \rightleftharpoons \text{ATP-CeO}^- + H_3O^+ + Na^+ \rightleftharpoons \text{ATP-CeONa} + H_2O + H^+ \quad (2)$$

TABLE-1
SOLUTION pH CHANGES BEFORE AND AFTER FLUORIDE ADSORPTION ONTO ATP-CeO_2 AT 25 °C

Initial fluoride concentration (mg/L)	Initial solution pH	Final solution pH
50	2.43	2.44
	3.10	3.34
	4.01	4.81
	4.96	5.82
	7.11	6.79
	8.17	7.51
	8.92	8.37
	10.04	9.73

In acidic environment, ATP-$CeOH_2^+$ were the main groups of the adsorbent surface and the fluoride ions were easily adsorbed on the adsorbent surface by electrostatic interaction and OH^- was released. At the same time, ATP-CeO^- on the adsorbent surface may also be complexed with the cations in solution and H^+ was released. However, the amount of OH^- released was much higher than H^+ released, which led to the increased pH after fluoride adsorption. In basic environment, ATP-CeO^- was the main groups on the adsorbent surface and the cations were easily adsorbed on the adsorbent surface and H^+ was released. Meanwhile, ATP-$CeOH_2^+$ also existed on the adsorbent surface and fluoride ions can also overcome the electric repulsion between fluoride ions and the negatively charged adsorbent surface and reach the adsorbent surface. Fluoride ions can also complex with ATP-$CeOH_2^+$ and OH^- was released. However, the amount of H^+ released was much higher that OH^- released, which resulted in decreased pH after fluoride adsorption. The results show that electrostatic interaction and anionic exchange contribute to the increased adsorption of fluoride ions onto ATP-CeO_2.

Effect of competing anions: The effect of added competing anions, Cl^-, NO_3^-, SO_4^{2-} and CO_3^{2-} on the adsorption of fluoride ions is given in Fig. 6. From the results, adsorption amount of fluoride ions onto ATP-CeO_2 decreased monotonously with increasing concentration of Cl^-, NO_3^-, SO_4^{2-} and CO_3^{2-}. The adsorption amount of fluoride ions decreased from 16.89 mg/g to 15.43, 13.86, 10.10 and 5.56 mg/g, respectively, when the initial concentration of Cl^-, NO_3^-, SO_4^{2-} and CO_3^{2-} was 25 mg/L. The effect of CO_3^{2-} on fluoride ions adsorption was more significant because CO_3^{2-} was a pH buffering agent and buffered the system pH to reduce the adsorption of fluoride or it wound compete with fluoride for active sorption sites[7]. Cl^- and NO_3^- have less impact on fluoride adsorption because Cl^- and NO_3^- formed outer-sphere surface complexes[31]. Overall, the impact of major anions on fluoride adsorption was in the order $CO_3^{2-} > SO_4^{2-} > Cl^- > NO_3^-$, which indicated that the presence of anions in solution would be competitive with aqueous fluoride ions for active sorption sites, thence, leading to the suppressed adsorption of fluoride ions.

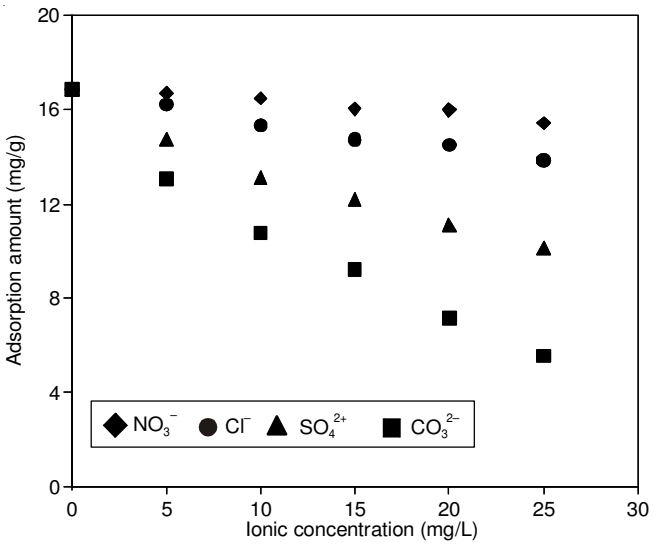

Fig. 6. Effect of ionic concentration of Cl^-, NO_3^-, SO_4^{2-} and CO_3^{2-} on fluoride adsorption onto ATP-CeO_2

Adsorption isotherms: The adsorption isotherm for fluoride onto ATP and ATP-CeO_2 at 15, 25 and 35 °C and pH 6 are shown in Fig. 7. From the result, fluoride adsorption onto ATP is less than 0.8 mg/g in tested range. Compared with the high adsorption amount of fluoride onto ATP-CeO_2, the adsorption amount of fluoride onto ATP is negligible and CeO_2 on the adsorbent surface contributes to the enhanced fluoride adsorption onto ATP-CeO_2. Additionally, fluoride adsorption onto ATP-CeO_2 increases with the initial fluoride concentration and increasing solution temperature, which

suggests that fluoride adsorption on the adsorbent surface is endothermic process.

To further understand the adsorption mechanism of fluoride onto ATP-CeO_2, Langmiur model and Freundlich model were used to simulate the adsorption experiment data. Generally, Langmuir model are frequently applied to describe the monolayer or homogeneous adsorption process, while Freundlich model is empirical in nature which supposes the adsorption is heterogeneous on the surface.

Langmuir model is expressed as follows:

$$q_e = \frac{q_m b C_e}{1 + b C_e} \quad (3)$$

Freundlich is expressed as follows:

$$q_e = K_f C e^{\frac{1}{n}} \quad (4)$$

where q_e (mg/g) is the equilibrium adsorption amount, C_e (mg/L) is the equilibrium concentration of fluoride ions, q_m (mg/g) is the theoretical adsorption capacity of adsorbent for fluoride ions, b (L/mg) is the affinity coefficient, K_f is Freundlich constant and 1/n is the heterogeneity factor.

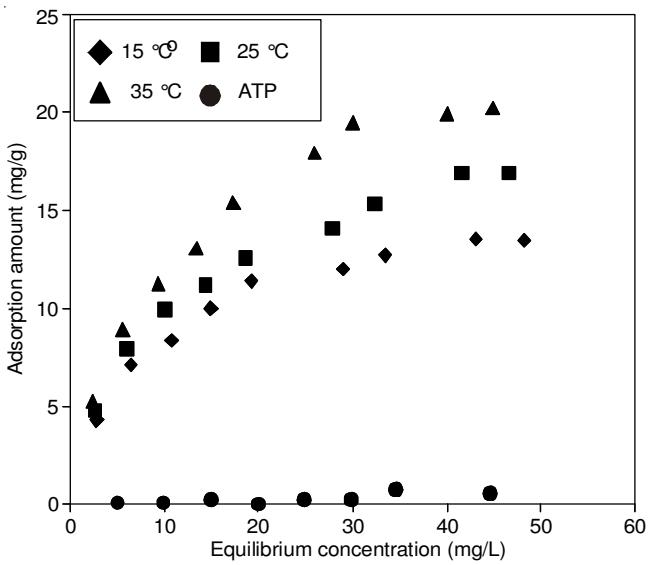

Fig. 7. Adsorption isotherms of fluoride onto ATP and ATP-CeO_2 at 15, 25 and 35 °C, respectively

The constants calculated from Langmuir model and Freundlich model are given in Table-2. It is obvious that the Langmuir model shows a better fit to the experimental data than Freundlich isotherms with a correlation coefficient of 0.99. The maximum adsorption capacity of ATP-CeO_2 calculated from Langmuir model are 14.97, 18.08 and 22.42 mg/g at 15, 25 and 35 °C, respectively, which is close to the experimental data. The present results suggest that the adsorption of fluoride onto ATP-CeO_2 surface is similar to be a monolayer or homogeneous adsorption. Separation factor R_L is the essential characteristic of Langmuir isotherm, which describes the feasibility of the adsorption process. The values of R_L calculated were 0.12-0.60 in tested range at 25 °C, indicating highly favorable adsorption of fluoride ions onto ATP-CeO_2.

Adsorption kinetics: To investigate the mechanism of adsorption, the pseudo-first-order adsorption and pseudo-second-order adsorption kinetic models were developed to test the adsorption kinetics data.

TABLE-2
LANGMUIR AND FREUNDLICH MODEL PARAMETERS FOR FLUORIDE ADSORPTION ON ATP-CeO_2 AT15, 25 AND 35 °C

Isotherm parameters	Temperature (°C)		
	15	25	35
Langmuir model parameters			
q_m (mg/g)	14.970	18.080	22.420
b (L/mg)	0.143	0.136	0.128
R^2	0.994	0.993	0.990
Freundlich model parameters			
n	2.560	2.350	2.170
K_f	3.240	3.500	3.880
R^2	0.963	0.983	0.981

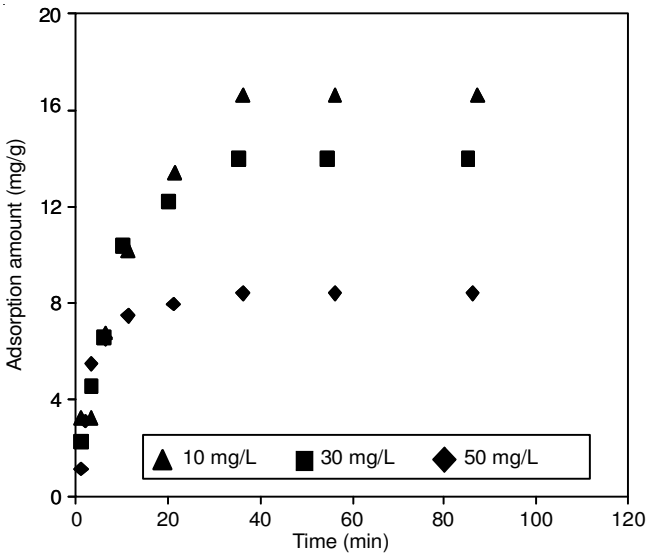

Fig. 8. Adsorption kinetics of fluoride adsorption onto ATP-CeO_2 at initial fluoride concentration of 10, 30 and 50 mg/L, respectively

The pseudo-first-order kinetics model is given as:

$$\log (q_e - q_t) = \log q_e - \frac{k_1}{2.303} t \quad (5)$$

The pseudo-second-order kinetics model is expressed as:

$$\frac{t}{q_t} = \frac{1}{k_2 q_e^2} + \frac{1}{q_e} t \quad (6)$$

wehere q_e is the equilibrium adsorption amount, mg/g, q_t is the adsorption amount at time *t*, mg/g and k_1, k_2 is pseudo-first-order and pseudo-second-order rate constant, respectively.

Adsorption kinetics of fluoride onto ATP-CeO_2 at initial fluoride concentration of 10, 30 and 50 mg/L and 25 °C are shown in Fig. 8. From the results, adsorption amount of fluoride onto ATP-CeO_2 increased with adsorption time and all got to adsorption equilibrium within 40 min. The simulated parameter based on the pseudo-first-order and pseudo-second-order model was tabulated in Table-3. From the results, the correlation coefficient values for pseudo-second-order model are significantly greater than those for pseudo-first-order model. Moreover, the theoretical adsorption capacity calculated from pseudo-second-order model are almost identical to the experimental values, further suggesting that fluoride adsorption onto ATP-CeO_2 obeys pseudo-second-order kinetics. The

adsorption rate constants of pseudo-second-order kinetics are 5.1×10^{-2}, 1.6×10^{-2}, 1.3×10^{-2} g/(mg.min) at initial fluoride concentration of 10, 30 and 50 mg/L, respectively, indicating of relatively slow adsorption process at a high initial fluoride concentration. This may be because that at low fluoride concentration, the ATP-CeO_2 surface is bare and fluoride ions in solution are easily found the active sites onto the adsorbent surface and anchored onto the adsorbent surface. At high fluoride concentration, most of the active sites of the adsorbent have been occupied and fluoride ions to be adsorbed must overcome the repulsion between fluoride ions in solution and fluoride ions adsorbed, which contributed to the suppressed fluoride adsorption.

TABLE-3
SIMULATED PARAMETERS OF FLUORIDE ADSORPTION ONTO ATP-CeO_2 BY PSEUDO-FIRST ORDER AND PSEUDO-SECOND ORDER KINETIC MODELS

Kinetics parameters	Initial fluoride concentration (mg/L)		
	10	30	50
q_{exp} (mg/g)	8.40	13.96	16.59
Pseudo-first order kinetics			
q_{cal} (mg/g)	5.24	12.76	13.52
k_1(1/min)	1.3×10^{-1}	9.5×10^{-2}	6.9×10^{-2}
R^2	0.923	0.973	0.991
Pseudo-second order kinetics			
q_{cal} (mg/g)	8.52	14.66	16.95
k_2(g/mg min)	5.1×10^{-2}	1.6×10^{-2}	1.3×10^{-2}
R^2	0.999	0.999	0.998

Desorption and readsorption capacity of the adsorbent: ATP-CeO_2 showed the low adsorption amount for fluoride in aqueous solution at alkaline solution, which reflected that fluoride saturated ATP-CeO_2 may be desorbed in alkaline solution. Therefore, 0.1 mol/L NaOH was chosed as desorbed agent. The readsorption capacity of regenerated ATP-CeO_2 studies shows that fluoride adsorption amount onto ATP-CeO_2 decreased from 16.90 mg/g to 15.20, 14.18, 12.96 and 12.34 mg/g, respectively, in four adsorption-regeneration cycles. The slight decrease of fluoride adsorption onto the regenerated adsorbent was observed in last two adsorption-regeneration cycles and the adsorbent still possesses high adsorption capacity for aqueous fluoride.

Conclusion

In this study, attapulgite supported CeO_2 composites were prepared and characterized by FTIR, XRD, TEM and zeta potential measurement. ATP-CeO_2 exhibits high adsorption amount for fluoride in aqueous solution and fluoride adsorption was highly dependent on solution pH and ionic strength. Electrostatic interaction and ionic exchange contribute to fluoride adsorption onto ATP-CeO_2. After adsorbed, fluoride saturated ATP-CeO_2 can be easily desorbed in alkaline solution and regenerated adsorbent still shows high adsorption capacity for fluoride in water, which implies that ATP-CeO_2 can be used as a recyclable adsorbent for the removal of fluoride in water and wastewater.

ACKNOWLEDGEMENTS

This work was supported by National Science Foundation of China (21107065), Natural Science Basic Research Plan in Shaanxi Province of China (2012JQ2003), Xi'an and the State Key Laboratory Program of Pollution Control and Resources Reuse (PCRRF11012), Nanjing, P.R. China.

REFERENCES

1. M. Sujana, A. Mishra and B. Acharya, *Appl. Surf. Sci*., **270**, 767 (2013).
2. X. Liao and B. Shi, *Environ. Sci. Technol*., **39**, 4628 (2005).
3. D. Santhi, *Asian J. Chem*., **18**, 707 (2006).
4. M. Tahaikt, R. El Habbani, A. Ait Haddou, I. Achary, Z. Amor, M. Taky, A. Alami, A. Boughriba, M. Hafsi and A. Elmidaoui, *Desalination*, **212**, 46 (2007).
5. B.D. Turner, P. Binning and S. Stipp, *Environ. Sci. Technol*., **39**, 9561 (2005).
6. X. Wu, Y. Zhang, X. Dou and M. Yang, *Chemosphere*, **69**, 1758 (2007).
7. M.S. Onyango, Y. Kojima, O. Aoyi, E.C. Bernardo and H. Matsuda, *J. Colloid Interf. Sci.*, **279**, 341 (2004).
8. F. Durmaz, H. Kara, Y. Cengeloglu and M. Ersoz, *Desalination*, **177**, 51 (2005).
9. Z. Amor, B. Bariou, N. Mameri, M. Taky, S. Nicolas and A. Elmidaoui, *Desalination*, **133**, 215 (2001).
10. F. Shen, X. Chen, P. Gao and G. Chen, *Chem. Eng. Sci*., **58**, 987 (2003).
11. A. Daifullah, S. Yakout and S. Elreefy, *J. Hazard. Mater*., **147**, 633 (2007).
12. N.A. Medellin-Castillo, R. Leyva-Ramos, R. Ocampo-Perez, R.F. Garcia de la Cruz, A. Aragon-Piña, J.M. Martinez-Rosales, R.M. Guerrero-Coronado and L. Fuentes-Rubio, *Ind. Eng. Chem. Res*., **46**, 9205 (2007).
13. M.S. Onyango, Y. Kojima, D. Kuchar, S.O. Osembo and H. Matsuda, *J. Chem. Eng. Jpn*, **38**, 701 (2005).
14. P. Liu and T. Wang, *J. Hazard. Mater*., **149**, 75 (2007).
15. H. Chen and A. Wang, *J. Hazard. Mater*., **165**, 223 (2009).
16. J. Zhang and A. Wang, *J. Chem. Eng. Data*, **55**, 2379 (2010).
17. J. Zhang, S. Xie and Y.S. Ho, *J. Hazard. Mater*., **165**, 218 (2009).
18. G. Zhang, Z. He and W. Xu, *Chem. Eng. J*., **183**, 315 (2012).
19. H. Liu, S.B. Deng, Z.J. Li, G. Yu and J. Huang, *J. Hazard. Mater*., **179**, 424 (2010).
20. L. Chen, T.J. Wang, H.X. Wu, Y. Jin, Y. Zhang and X.M. Dou, Powder Technol., 206, 291 (2011).
21. L. Chen, H.X. Wu, T.J. Wang, Y. Jin, Y. Zhang and X.M. Dou, *Powder Technol*., **193**, 59 (2009).
22. H.X. Wu, T.J. Wang, L. Chen, Y. Jin, Y. Zhang and X.M. Dou, *Ind. Eng. Chem. Res*., **48**, 4530 (2009).
23. S. Deng, H. Liu, W. Zhou, J. Huang and G. Yu, *J. Hazard. Mater*., **186**, 1360 (2011).
24. Z.C. Di, Y.H. Li, X.J. Peng, Z.K. Luan and J. Liang, *Solid State Phenomena*, **121-123**, 1221 (2007).
25. Z.J. Li, S.B. Deng, X.Y. Zhang, W. Zhou, J. Huang and G. Yu, *Front. Environ. Sci. Eng. China*, **4**, 414 (2010).
26. F. Luo and K. Inoue, *Solvent Extr. Ion Exch*, **22**, 305 (2004).
27. N. Viswanathan and S. Meenakshi, *J. Appl. Polym. Sci*., **112**, 1114 (2009).
28. Y.M. Xu, A.R. Ning and J. Zhao, *J. Colloid Interf. Sci*., **235**, 66 (2001).
29. X.R. Yan, K.X. Song, J.P. Wang, L.C. Hu and Z.H. Yang, *J. Rare Earths*, **16**, 275 (1998).
30. Z. Chen, F. Chen, X. Li, X. Lu, C. Ni and X. Zhao, *J. Rare Earths*, **28**, 566 (2010).
31. A. Tor, Y. Cengeloglu, M.E. Aydin and M. Ersoz, *J. Colloid Interf. Sci*., **300**, 498 (2006).